STOCHASTIC MODELLING FOR THE MAINTENANCE OF LIFE CYCLE COST OF RAILS USING MONTE CARLO SIMULATION

Rick Vandoorne

University of Pretoria, Department of Civil Engineering, South Africa

rick.vandoorne@up.ac.za

Petrus Johannes Gräbe

University of Pretoria, Department of Civil Engineering, South Africa

hannes.grabe@up.ac.za

Abstract: The need for decision support systems to guide maintenance and renewal (M&R) decisions for infrastructure is growing due to tighter budget requirements and the concurrent need to satisfy reliability, availability and safety requirements. The rail of the railway track is one of the most important components of the entire track structure and can significantly influence maintenance costs throughout the life cycle of the track. Life cycle cost (LCC) estimation is a popular decision support system. A calculated LCC has inherent uncertainty associated with the reliability of the input data used in such a model. A stochastic LCC model was developed for the rail of the railway track incorporating imperfect inspections. The model was implemented using Monte

Carlo simulation in order to allow quantification of the associated uncertainty within the LCC calculated. For a given set of conditions an optimal renewal tonnage exists at which the rail should be renewed in order to minimise the mean LCC. The optimal renewal tonnage and minimum attainable mean LCC are dependent on inspection interval length, weld type used for maintenance as well as the cost of maintenance and inspection activities. It was found that the distribution of LCC for a fixed renewal tonnage followed a Lognormal probability distribution. The standard deviation of this distribution can be used as a metric to quantify uncertainty. Uncertainty increases with an increase in inspection interval length for a fixed rail renewal tonnage. With all other conditions fixed, it was found that LCC uncertainty increases with an increase in the rail renewal tonnage. The relative contribution of uncertainty of the planned and unplanned maintenance costs towards the total LCC uncertainty was found to be dependent on the inspection interval length.

Keywords: Maintenance, Monte Carlo, life cycle cost, uncertainty, rail, modelling

INTRODUCTION

The rail remains one of the most important components of the entire railway operation (1). Maintenance and renewal (M&R) decisions largely dictate the performance of the rail throughout its life cycle as well as the associated life cycle cost (LCC) achieved. Therefore, it is beneficial to have a decision support system (DSS) which can quantitatively justify M&R decisions based on their associated LCC (2). Operational delays and derailments are caused when a rail failure occurs. Delay costs resulting from in-service failures have been shown to increase exponentially with daily traffic

volume (3). A rail failure is defined as the termination of the ability of the rail to perform its functions (4). The functions of the rail are summarised by Esveld (2001) (1).

RAIL FATIGUE DEFECTS

Defect Classification

Rail defect and damage nomenclature is poorly standardised, partly due to the fact that many rail damage mechanisms are interrelated. A rail damage hierarchy suggested by Reinschmidt et al. (2015) (5) is presented in Figure 1.The focus of this study is on rolling contact fatigue (RCF) damage which can be sub-divided into surface- and subsurface-initiated RCF defects. This study does not include any form of thermal loading, wear or shock type damage from extreme physical loading scenarios.

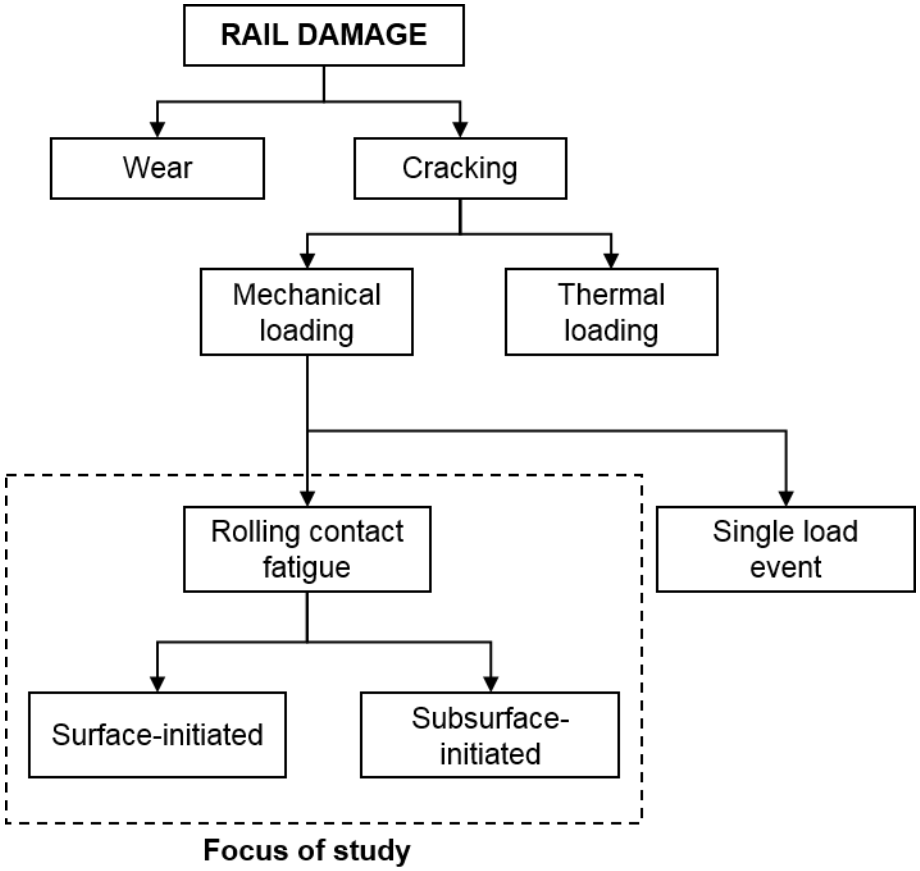

Figure 1. Rail damage hierarchy (5)

Fröhling (2007) (6) classifies rail deterioration into a wear regime and a stress regime. This is similar to the classification in Figure 1. Rail deterioration tends to be governed by the stress regime for high axle loads as experienced on heavy haul lines. Therefore, the model developed for this study would be most applicable to a heavy haul scenario. Deterioration in the stress regime is difficult to measure, control and predict (6). Thus, a stochastic procedure is often adopted to model rail deterioration related to fatigue. Rail fatigue defects can be further classified as follows (7):

- Defects related to rail joints such as welds
- Defects related to rail quality

Some common rail fatigue defects related to rail quality are (8):

- Shelling
- Tache ovale or kidney defects
- Head checks
- Squats
- Spalling

For an in-depth discussion on these and other rail fatigue defects the reader is referred to Kumar (2006) (8) and Reinschmidt et al. (2015) (5). For the purpose of this study, defects at the rail joints are simply classified according to whether they occur at an alumino-thermic weld (ATW) or a flash butt weld (FBW). When a defect is removed or a rail failure repaired, a closure rail is installed and joined to the existing rail using welds. Therefore, the number of welds present in a representative km of rail will likely increase with the cumulative tonnage borne by the rail as a system.

Defect Initiation, Propagation and Rail Failure

A fatigue initiated rail defect may experience 3 stages as it progresses to ultimate rail failure, namely (9):

1. A fatigue crack or defect must be present within the rail.
2. The fatigue crack grows in size with loading cycles.
3. The rail ultimately fails if the fatigue crack is not maintained and reaches a critical defect size.

An anomaly in the rail is termed a potential failure or defect once it is large enough to be detected by modern ultrasonic, eddy current, magnetic particle or wave inspection technology (10). Therefore, it is assumed that any anomalies which cannot be detected do not pose a risk to the functioning of the rail. The time from when a defect initiates until the time it causes a functional failure is termed the P-F interval (11). Defect growth and critical defect size at failure for transverse rail fatigue defects were studied by Jeong et al. (1997) (12) using a fracture mechanics approach. It was determined that critical defect size at failure was a function of the bending, thermal and residual stress within the rail. The location of the defect within the profile and the fracture toughness of the steel also influence the critical defect size. The rate of growth of rail fatigue defects is dependent on the initial defect size as well as the rail temperature. Furthermore, crack growth rates have been found to be significantly influenced by the loading stress spectra as well as the curvature of the track segments (13). Due to the variability in the initiation, growth rate and critical defect size of rail fatigue defects, a stochastic rather than a deterministic modelling approach is recommended for use in a life cycle cost analysis (LCCA). This variability in the reliability and maintainability parameters required to conduct a LCCA translates to uncertainty in the final LCC estimation.

MAINTENANCE MODELLING

In general, maintenance actions can be classified as either corrective maintenance (CM) or preventive maintenance (PM). CM is defined as any action performed as a result of failure in order to restore the system to a specified condition whereas PM is defined as all actions performed in an attempt to mitigate failure (14). Therefore, CM is performed when a rail fails and PM actions include rail grinding, rail inspection and

the removal of a defect once detected before failure occurs. PM can be further classified as being either routine-based or condition-based. Rail grinding and inspection are generally routine-based whereas removal of detected defects is considered a condition-based PM action.

In maintenance modelling it is common to use a hazard function $\lambda(t)$ (also called a failure rate function or the force of mortality) to describe the arrival of defects or failures. A hazard function $\lambda(t)$ is defined such that $\lambda(t) \cdot dt$ represents the probability that a component's life will end in the time interval $(t, t + dt]$ given that it has survived up to age t (15). Maintenance modelling can be divided into 5 different categories according to the effect the maintenance action has on the hazard rate of the system modelled (16). These 5 categories are shown in Table 1.

Table 1. Maintenance modelling types classified according to their effect on the system hazard rate (16)

Repair type	Effect on hazard rate of system	Layman's description
Perfect maintenance	Decreases to same value as when new	As good as new
Imperfect maintenance	Decreases but not to same value as when new	Between good as new and bad as old
Minimal maintenance	Not affected	As bad as old
Worse maintenance	Increases	Worse than old
Worst maintenance	N/A	Instant failure

The mechanism by which rail fatigue defects initiate and grow is related to the loading cycles experienced by the rail. Thus, fatigue defects are best modelled with respect to the gross tonnage borne by the rail measured in million gross tonnes (MGT) rather than time.

Uncertainty

The objective of this study was to quantify the uncertainty present in LCC estimation as a DSS. A stochastic procedure allows one to take into account the variability present in the reliability and maintainability parameters. Uncertainty in the reliability and maintainability parameters is classified as Level 2 uncertainty by Patra et al. (2009) (16) and is the focus of this study. Level 1 uncertainty is related to uncertainty in the train delay costs, possible penalty costs and derailment costs and is not considered in this study. Patra et al. (2009) (17) studied the effects of variability in mean time to failure (MTTF) and mean time to repair (MTTR) on the LCC associated with the M&R of the high and low rail of curves of different radii. It is understood that the Bootstrap Method was used to calculate confidence intervals for the MTTF and MTTR. The Point Estimation Method (PEM) was then used to infer corresponding point estimates for the LCC. However, a limitation to the use of the PEM is that the LCC must be expressible as a closed-form solution. This restricts the complexity of the LCC estimation method and often calls for further limiting assumptions to be made which could affect the accuracy of the LCC estimation.

A Stochastic Rail Defect Model from the Literature

Zhao et al. (2006) (10) developed a stochastic LCC model for rail, incorporating imperfect inspections. Using their model, an optimal inspection interval can be found at which a minimum expected LCC can be achieved under a given set of conditions. The model distinguishes between two different types of defects, namely: Type A defects which are ATW defects and Type B defects which are all other defects and include FBW defects, tache ovale defects and squat defects. The hazard function of

Type A defects must be specified for a single ATW whereas the hazard function of Type B defects must be specified in proportion to the length of the rail modelled. It is counter intuitive that the hazard function of FBWs is specified in proportion to the length of rail modelled because FBWs are physically countable phenomena whereas all other Type B defects are not countable until such a point that the defect physically arises. Defects are categorised in this manner by Zhao et al. (2006) (10) because maintenance of a Type A defect will introduce 1 additional ATW into the system whereas maintenance of a Type B defect will introduce 2 additional ATWs into the system. The novelty in the research by Zhao et al. (2006) (10) is that their model accounts for an increasing hazard rate of Type A defects due to maintenance. This is caused by the fact that the number of ATWs in the system will increase as maintenance is conducted through the installation of a closure rail. Two important assumptions of the model can be summarised as follows:

- Maintenance is modelled using minimal maintenance as defined in Table 1.
- The hazard function of FBWs remains unaffected by maintenance activities meaning that the modelled system essentially does not sense the effect of replacing FBWs with ATWs during maintenance.

NUMERICAL MODEL

The numerical model developed for this study and programmed using MATLAB, is described in this section. The basic assumptions with regard to the modelling procedure may be summarised as follows:

- Rail defect arrival tonnages are modelled using the hazard function of the 2-parameter Weibull distribution. Use of the Weibull distribution to model rail

defects is supported by Zarembski (1991) (18), Zhao et al. (2006) (10) and studies highlighted by Roth (2008) (19).

- Defect inter-arrival tonnages t_d are assumed to be independent and identically distributed and thence follow a non-stationary exponential probability distribution with a mean value function specified by the hazard function of the Weibull distribution. This is sometimes referred to as the power law process.
- The P-F interval length t_{P-F} follows an exponential distribution as assumed by Zhao et al. (2006) (10).
- Each defect type j has a probability η_j of being detected upon ultrasonic inspection.
- The hazard rate of surface-initiated RCF defects is reduced by a factor γ to account for the effects of preventive rail grinding (20).
- There is no delay in any maintenance actions.
- The effect of maintenance on the hazard rate of weld defects is modelled using perfect maintenance.
- The welds used to join the closure rail to the existing rail during maintenance can be modelled as either ATWs of FBWs with their own respective hazard functions.

Defects are classified into Category A and Category B defects. Category A defects are defects related to the joining of the rail such as ATW and FBW defects and Category B defects are defects related to the quality of the rail (not at the joints). The hazard function of a Category A defect is specified in proportion to a single weld whilst the

hazard function of a Category B defect is specified in proportion to the length of modelled rail. For this study the rail of a single representative km of track is modelled.

The maintenance type of defects or failures in the model can be categorised as being either:

- Planned maintenance
- Unplanned maintenance
- Renewal maintenance

Planned maintenance occurs if a defect is found by an inspection activity. Unplanned maintenance occurs either if the defect is not detected during an inspection and ultimately causes a functional failure or if there is no opportunity for detection before the defect causes a functional failure. Renewal maintenance occurs either when no defect is present in a weld at the time of rail renewal of if a defect is present in the rail or weld but has not been detected or caused functional failure at the time of rail renewal.

The costs which are included in the model are:

- Renewal cost per km of modelled track, c_R
- Planned maintenance cost using either ATWs or FBWs, $c_{p_{ATW}}$ or $c_{p_{FBW}}$
- Unplanned maintenance cost using either ATWs or FBWs, $c_{f_{ATW}}$ or $c_{f_{FBW}}$
- Ultrasonic inspection cost per inspection per km of modelled track,c_I
- Rail grinding cost per grinding activity per km of modelled track, c_g

All the costs specified in the model must include labour, equipment and delay costs. Unplanned maintenance costs are larger than planned maintenance costs due to the traffic delay associated with unplanned maintenance. No discount rate was modelled. This assumption was also made by Zhao et al. (2006) (10) and Shafiee et al. (2016) (21). Furthermore, costs are assumed to remain constant throughout the life of the modelled rail. Although these assumptions may not represent reality, they allow for clearer analysis of the LCC uncertainty which arises from variability in the technical parameters rather than the economic parameters.

Sampling Random Variates

Monte Carlo simulation and the Inverse Transform Method were used to generate values of t_d and t_{P-F} with the desired probability distribution (22). The uniform random variable U, used to sample values of t_d and t_{P-F}, was generated using a Latin hypercube sample in order to ensure a uniform distribution with fewer required iterations. The inter-arrival tonnages t_d for defects are sampled using Equation 1 which is an inversion of the cumulative density function (CDF) of the exponential probability distribution with a mean value function given by the hazard function of the Weibull distribution:

$$t_d(U) = \left[a^{\alpha} - \frac{\beta^{\alpha} \ln(1-U)}{1-\gamma}\right]^{\frac{1}{\alpha}} - a \quad \textbf{(1)}$$

Where:

t_d = defect inter-arrival tonnage (MGT)

U = a random variate sampled from a uniform distribution in the interval $(0,1)$

α = the Weibull shape parameter for the defect type under consideration

β = the Weibull scale parameter for the defect type under consideration (MGT)

γ = the grinding reduction factor

a = a shifting parameter (MGT)

The shifting parameter is used to change the sampling distribution in order to model minimal maintenance. The value of a is equal to the cumulative tonnage at which the defect or failure was maintained for all Category B defects. However, the value of a is 0 for Category A defects modelled using perfect maintenance and is equal to the cumulative tonnage at which the weld was installed when using minimal maintenance. The origin of the shifting parameter a in Equation 1 is illustrated in Figure 2 which shows the hazard rate in relation to the age t of a newly installed weld. The hazard rate for the minimal maintenance case is for a value of a = 200 MGT.

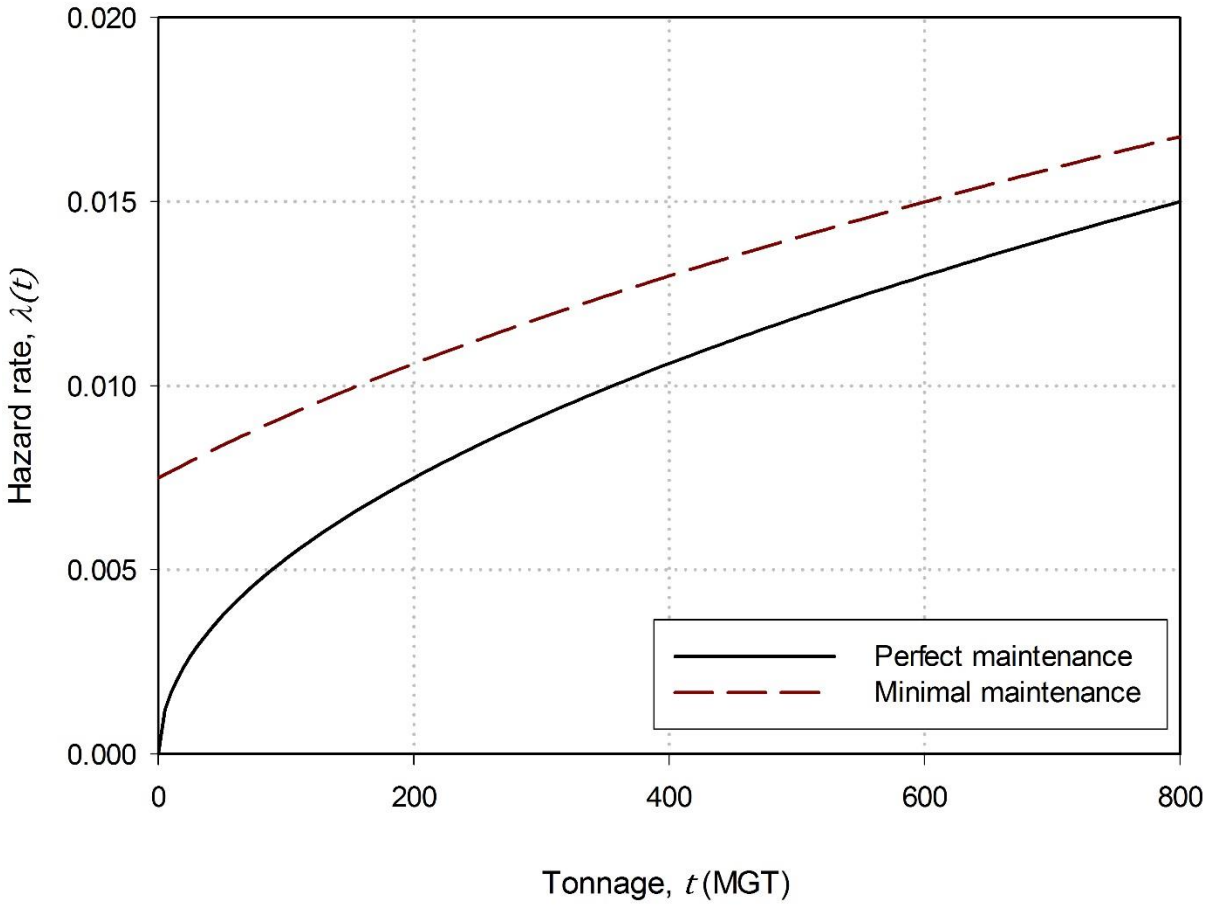

Figure 2. The hazard rate of a weld installed at a cumulative tonnage of 200 MGT using perfect maintenance and minimal maintenance

The P-F interval lengths for defects are sampled using Equation 2 which is the inversion of the CDF of an exponential distribution:

$$t_{P-F}(U) = -\mu \ln(1-U) \quad \textbf{(2)}$$

Where:

t_{P-F} = the P-F interval length (MGT)

U = a random variate sampled from a uniform distribution in the interval $(0,1)$

μ = expected P-F interval length for the defect type under consideration (MGT)

Procedural Logic

The logical of the developed numerical model is illustrated in Figure 3. An array of strictly increasing renewal tonnages $\overrightarrow{\boldsymbol{T_R}}$ is specified at which the model must calculate the associated LCCs. The calculation procedure begins by simulating a life cycle with a renewal tonnage equal to the last (and largest) renewal tonnage in the array $\overrightarrow{\boldsymbol{T_R}}_{end}$.

In Step 2, Category B defects are simulated using Monte Carlo sampling. The appropriate variables α, β and μ for the defect type under consideration (e.g. tache ovale defect or squat defect) are used during Step 2 within Equation 1 and 2 respectively to calculate t_d and t_{P-F} for each simulated Category B defect. Category B defects are simulated in a cumulative manner in Step 2 until such a point that the tonnage at which the defects start to occur become larger than T_R.

It is assumed that the arrival of Category B defects is independent of the number of welds and Category A defects in the system. Therefore, it follows implicitly that the quality of any closure rail installed during maintenance activities is the same as the existing rail to which it is welded.

Step 3 simulates the arrival and growth of Category A defects for welds present in the newly installed rail at T = 0 MGT. Defect inter-arrival tonnages t_d and P-F intervals t_{P-F} are calculated for each ATW $n_{0_{ATW}}$ and FBW $n_{0_{FBW}}$. Step 4 simulates the maintenance of the defects simulated in Steps 2 and 3. Maintenance of defects takes into account the cumulative tonnage at which the defect initiated T_d and at which it is

predicted to fail T_f. The number of inspections which will take place between T_d and T_f as well as Monte Carlo sampling is then used to determine whether the defect is detected (and planned maintenance takes place) or whether it remains undetected and causes a functional failure (and unplanned maintenance takes place). Two new welds are introduced to the system for every planned and unplanned maintenance action. The defective or failed weld is now considered inactive and no longer part of the system for the remainder of the simulation process. If the maintenance type is classified as renewal maintenance no new welds are introduced to the system. Handling of all Category B defects is now complete for the virtual life cycle under consideration.

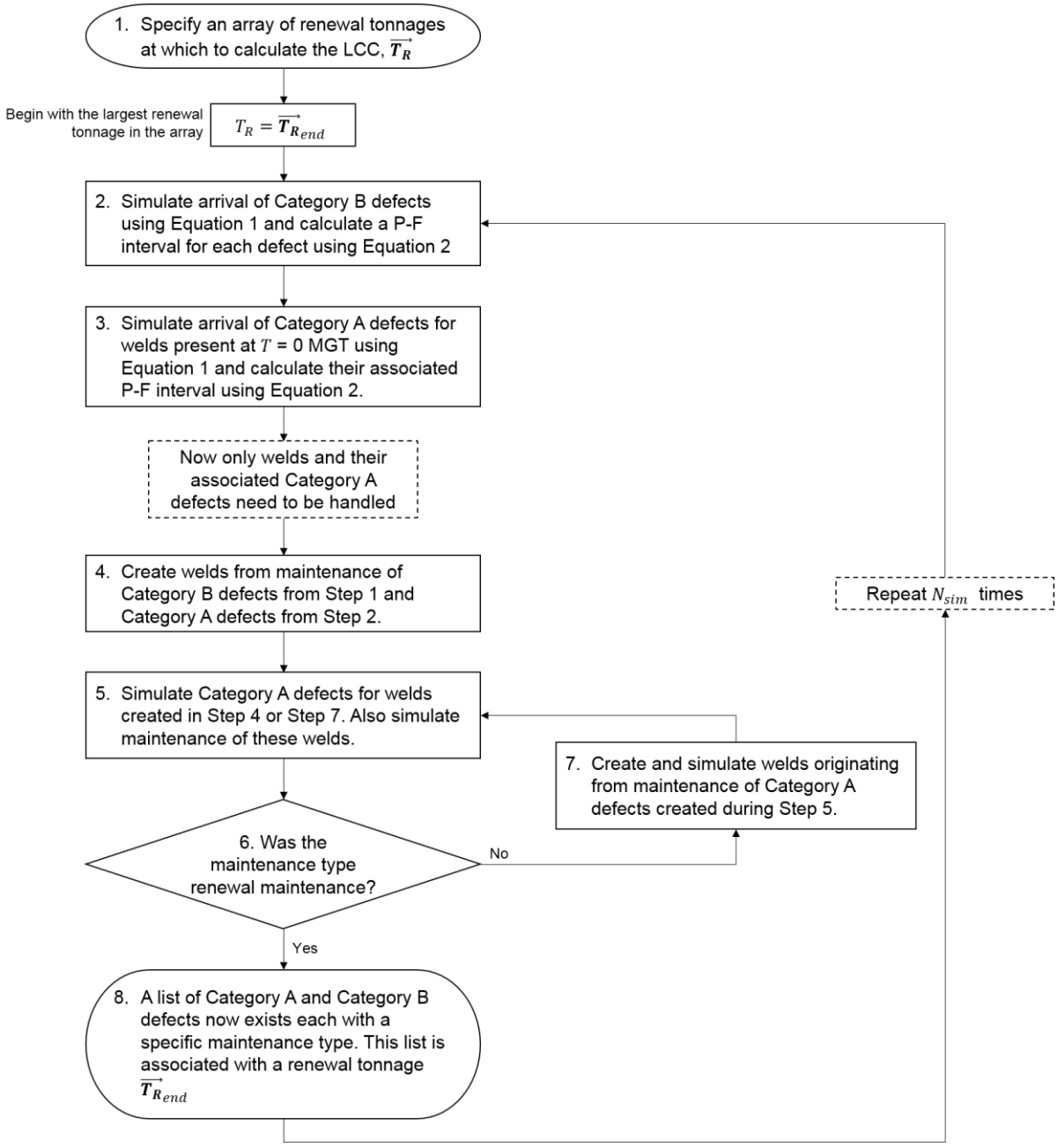

Figure 3. Illustration of procedural logic of the developed numerical model

Steps 5, 6 and 7 together form a loop which continues until the maintenance type of all active welds in the system are classified as renewal maintenance. Step 5 simulates the arrival and failure of defects for welds created in Step 4 or Step 7. Step 6 checks whether all the active welds in the system have been maintained with renewal

maintenance. If so, no new welds need to be created and the loop may be terminated. Otherwise, if planned and\or unplanned maintenance types exist within the active welds, new welds need to be created and the loop continued.

When the loop is terminated, the simulation procedure for a single virtual life cycle with renewal tonnage $\overrightarrow{\boldsymbol{T}_{\boldsymbol{R}_{end}}}$ is complete. A list of Category A and Category B defects now exists for a single virtual life cycle at renewal tonnage $\overrightarrow{\boldsymbol{T}_{\boldsymbol{R}_{end}}}$, each with an assigned maintenance type namely: planned maintenance, unplanned maintenance or renewal maintenance. The procedure is now repeated N_{sim} times to simulate N_{sim} virtual life cycles each with unique values of t_d and t_{P-F} and defect detection rates. Each virtual life cycle simulated has its own unique set of defects with associated maintenance types.

The defects for the remaining renewal tonnages in $\overrightarrow{\boldsymbol{T}_{\boldsymbol{R}}}$ must now be determined. This is done through a process of truncation and modification of the maintenance types. The defects associated with renewal tonnage $\overrightarrow{\boldsymbol{T}_{\boldsymbol{R}_{end}}}$ are truncated according to whether the defect would have existed at the other renewal tonnages in $\overrightarrow{\boldsymbol{T}_{\boldsymbol{R}}}$. The maintenance types for each defect are also modified according to whether a planned or unplanned maintenance activity now becomes a renewal maintenance activity due to the smaller renewal tonnage. At the end of this stage of the simulation, a unique set of defects will exist for each simulated life cycle, corresponding to each renewal tonnage in $\overrightarrow{\boldsymbol{T}_{\boldsymbol{R}}}$.

Cost Calculation

The LCC for virtual life cycle N at renewal tonnage $\overrightarrow{\boldsymbol{T_{R_i}}}$, $\overrightarrow{\boldsymbol{c_{LCC}}}_{N,i}$ is subsequently calculated using the list of defects and their associated maintenance types as shown in Equation 3:

$$\overrightarrow{\boldsymbol{c_{LCC}}}_{N,i} = \frac{\left(c_R + n_{I_i} c_I + n_{g_i} c_g + c_p n_{p_i} + c_f n_{f_i}\right)}{\overrightarrow{\boldsymbol{T_{R_i}}}} \quad \textbf{(3)}$$

Where:

n_{p_i} = the number of planned maintenance activities during the tonnage interval $(0, \overrightarrow{\boldsymbol{T_{R_i}}})$

n_{f_i} = the number of unplanned maintenance activities during the tonnage interval $(0, \overrightarrow{\boldsymbol{T_{R_i}}})$

n_{I_k} = the quantity of ultrasonic inspections conducted during the tonnage interval $(0, \overrightarrow{\boldsymbol{T_{R_i}}})$

n_{g_k} = the quantity of grinding activities conducted during the tonnage interval $(0, \overrightarrow{\boldsymbol{T_{R_i}}})$

$\overrightarrow{\boldsymbol{T_{R_i}}}$ = the i^{th} renewal tonnage in the renewal tonnage array $\overrightarrow{\boldsymbol{T_R}}$

$\overrightarrow{\boldsymbol{C_{LCC}}}$ is a two-dimensional array in which each row corresponds to virtual life cycle N and each column to a specific renewal tonnage in $\overrightarrow{\boldsymbol{T_R}}$. All costs are normalised against the tonnage borne by the rail. Therefore, if a single km of rail is modelled, the associated LCC will be expressed in units of cost/MGT/km.

ANALYSIS AND DISCUSSION OF RESULTS

A reference case analysis is defined with parameters as shown in Table 2 through 4. This is done so that the entire parameter set does not have to be redefined for each set of results shown. The parameters in Table 2 and 4 are taken from Zhao et al. (2006) (10) where applicable. The costs in Table 3 are representative of typical costs for a South African Heavy Haul scenario.

Table 2. Stochastic input parameters used for the reference case analysis

Defect	α	β (MGT)	μ (MGT)	η
ATW defects	1.01	315.8	10	0.7
FBW defects	2.00	286.6	10	0.7
Squat defects	2.50	191.8	5	0.6
Tach ovale defects	2.17	182.3	7	0.7

Table 3. Cost parameters used for the reference case analysis

Cost parameter	Symbol	Value
Planned repair cost using ATWs per defect	$c_{p_{ATW}}$	R 16 000.00
Unplanned repair cost using ATWs per failure	$c_{f_{ATW}}$	R 115 000.00
Ultrasonic inspection cost per km	c_I	R 2 400.00
Rail grinding cost per km	c_g	R 45 000.00
Rail renewal cost per km	c_R	R 2 050 000.00

Table 4. Deterministic input parameters used for the reference case analysis

Parameter	Symbol	Value
Ultrasonic inspection interval (MGT)	s_I	2.5
Rail grinding interval (MGT)	s_g	10.0
Initial number of ATWs	$n_{0_{ATWs}}$	0
Initial number of FBWs	$n_{0_{FBWs}}$	22
Hazard rate reduction factor due to rail grinding	γ	0.4
Number of simulated life cycles	N_{sim}	20 000
Weld type used for maintenance	-	ATW
Maintenance modelling type	-	Perfect maintenance

A bivariate histogram of LCC c_{LCC} versus renewal tonnage T_R is shown in Figure 4. Normal, lognormal and Weibull probability distributions were fitted to the data at varying inspection interval lengths s_I for a fixed renewal tonnage of T_R = 800 MGT. A Pearson Chi-square goodness-of-fit hypothesis test was conducted to determine the most appropriate probability distribution to describe the data. The number of bins used was set to $2(n_{data})^{\frac{2}{5}}$ rounded to the nearest integer, with n_{data} equal to the number of data points used for the hypothesis test. The bin edges were determined such that each bin is equiprobable under the hypothesised distribution (23). The P-values of the tests are summarised in Table 5. It is clear from the significantly higher P-values (which are desirable) that the lognormal probability distribution best describes the distribution of the LCC c_{LCC} for a given renewal tonnage T_R. The fitted lognormal distributions for the reference case analysis are shown plotted over the bivariate histogram in Figure 4.

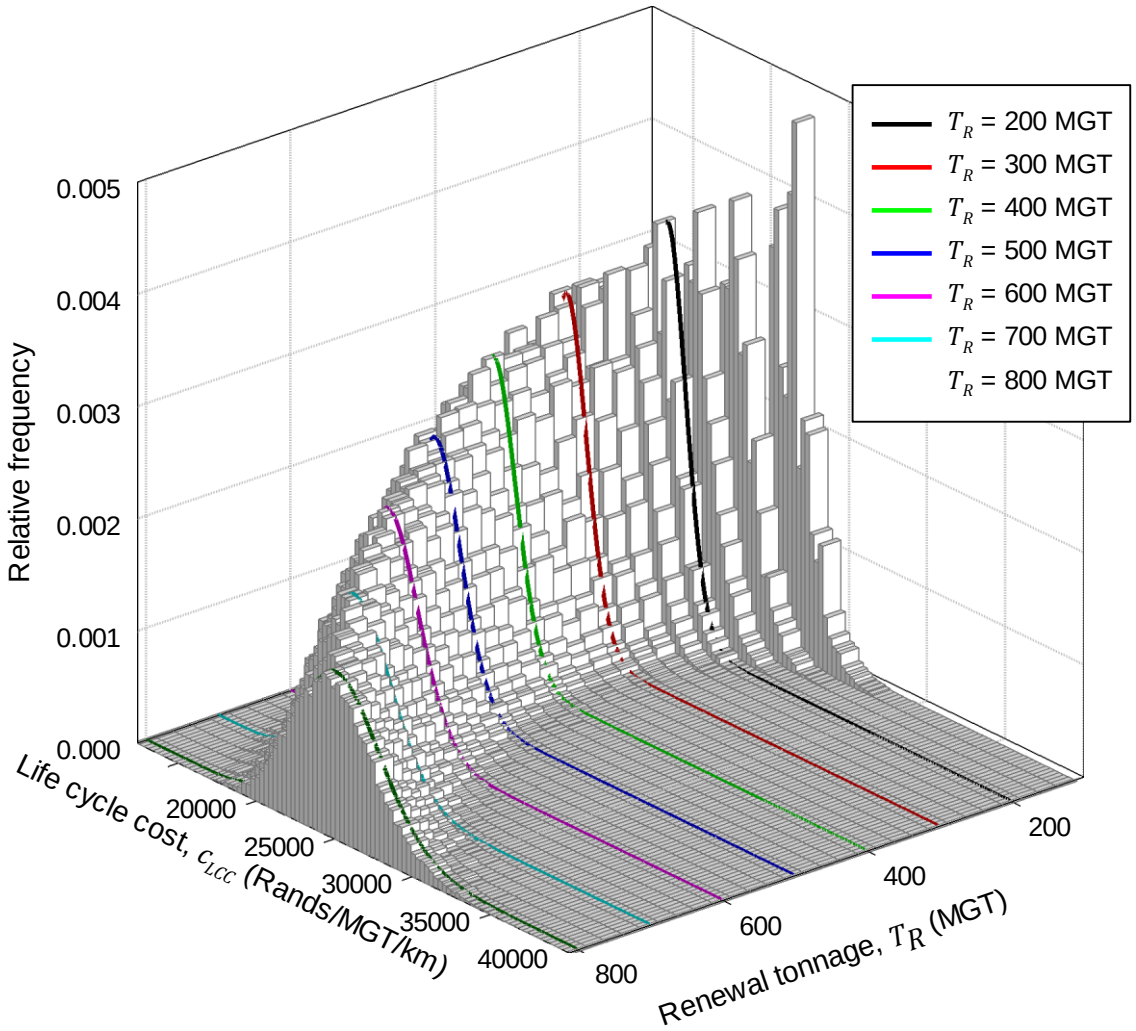

Figure 4. Bivariate histogram showing the probability of attaining a given LCC c_{LCC} at a particular renewal tonnage T_R with the fitted lognormal distributions shown

Table 5. P-value for fitted distributions at varying inspection interval lengths s_I for T_R = 800 MGT

Inspection interval length, s_I (MGT)	Normal	Lognormal	Weibull
0.1	4.68×10^{-40}	7.48×10^{-15}	0
0.5	1.21×10^{-29}	0.064	0
1.0	4.99×10^{-28}	0.951	0
2.5	2.22×10^{-41}	0.116	0
5.0	4.13×10^{-35}	0.488	0
10.0	1.03×10^{-30}	0.068	0
20.0	3.11×10^{-27}	0.521	0

The bivariate histogram in Figure 4 viewed in the c_{LCC} – relative frequency plane at T_R = 400 MGT produces the plot in Figure 5 (a). If the mean LCC $\overline{\boldsymbol{c_{LCC}}}$ is calculated for each renewal tonnage in $\overrightarrow{\boldsymbol{T_R}}$ then the plot in Figure 5 (b) is produced, analogous to the results obtained by Zhao et al. (2006) (10). The mean LCC plot does not provide any information with regard to the LCC uncertainty at a given renewal tonnage. The minimum mean LCC $\overline{\boldsymbol{c_{LCC}}}_{min}$ and the renewal tonnage at which it occurs $T_{R_{cr}}$ are shown in Figure 5 (b).

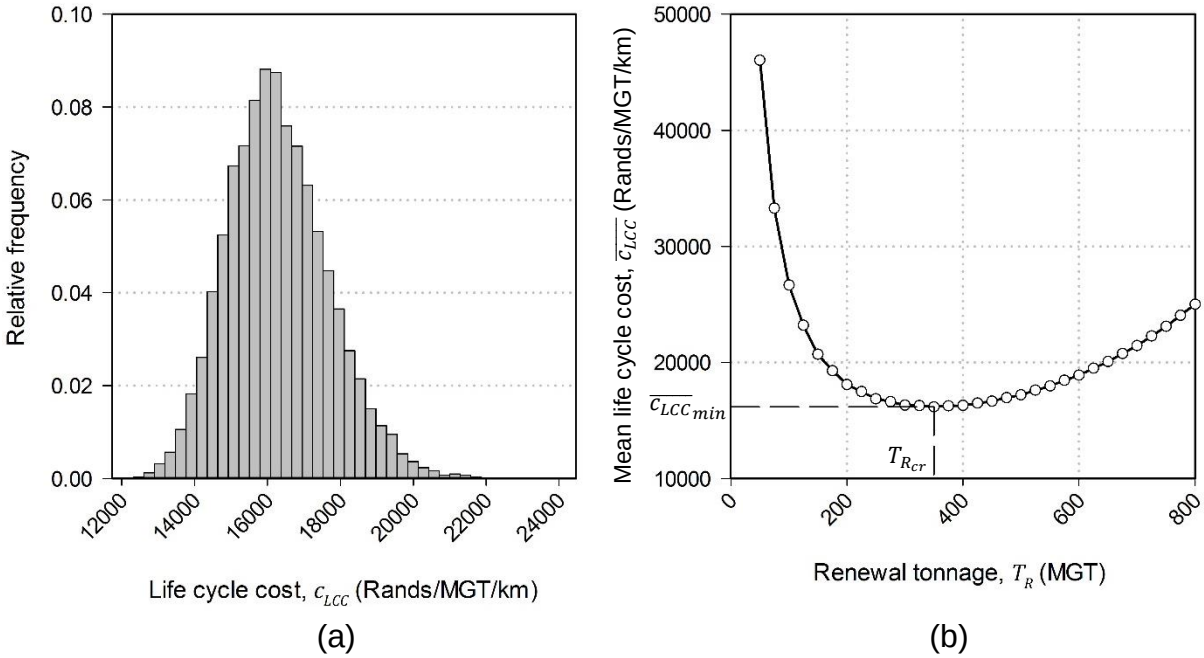

(a) (b)

Figure 5. (a) Distribution of LCC c_{LCC} at a renewal tonnage T_R = 400 MGT (b) Mean LCC $\overline{c_{LCC}}$ versus renewal tonnage T_R

In order to attain some sense for the LCC uncertainty present, the mean LCC curve may be plotted with its corresponding 1st and 99th percentiles. Figure 6 illustrates plots of the mean LCC $\overline{\boldsymbol{c_{LCC}}}$ versus renewal tonnage with the corresponding percentiles plotted using dashed lines for inspection interval lengths of s_I = 0.1 and 5.0 MGT. It is evident from the diverging nature of the 1st and 99th percentile plots that the variability

in the LCC c_{LCC} increases with renewal tonnage T_R. Furthermore, the distance between the 1st and 99th percentile for a fixed renewal tonnage is larger for an inspection interval length s_I = 5.0 MGT than for an inspection interval length s_I = 0.1 MGT. This suggests that uncertainty increases with both an increase in renewal tonnage T_R as well as with an increase in inspection interval length s_I.

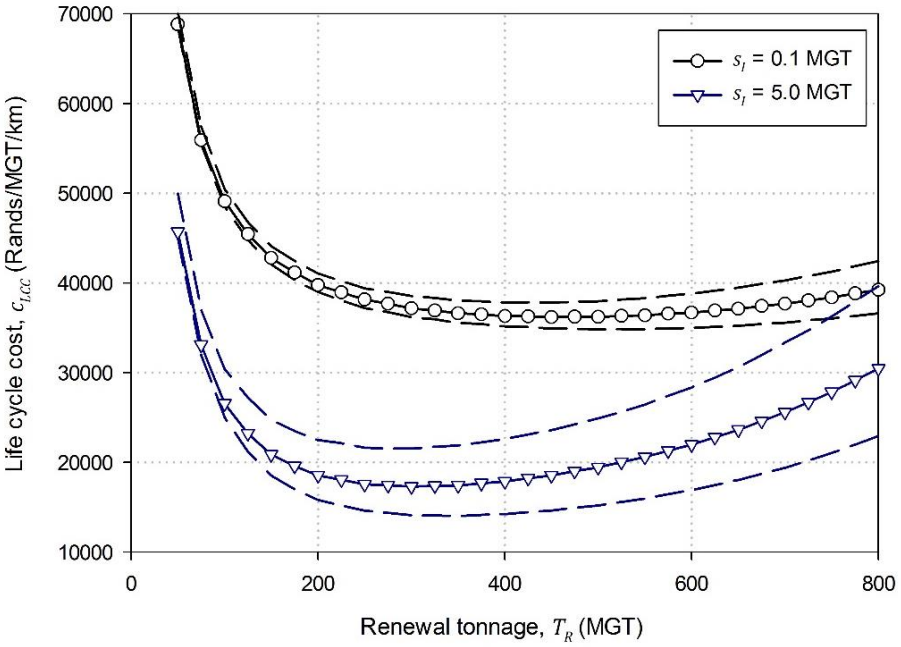

Figure 6. Mean LCC $\overline{c_{LCC}}$ versus renewal tonnage T_R for s_I = 0.1 and 5.0 MGT, indicating the 1st and 99th percentiles

To quantify the observed uncertainty trends, the standard deviation of the LCC σ_{LCC} at a fixed renewal tonnage is used as a suitable metric. The LCC uncertainty σ_{LCC} versus renewal tonnage T_R is plotted in Figure 7 for varying inspection interval lengths s_I. From Figure 7 it is clear that the uncertainty in the LCC σ_{LCC} increases with an increase in renewal tonnage T_R for all inspection interval lengths s_I considered in this study. Furthermore, the plots in Figure 7 appear to have inflection points, the location of which are dependent on the inspection interval length s_I. After this inflection point, the rate

of change in LCC uncertainty σ_{LCC} becomes positive, demonstrating a rapid increase in uncertainty as the renewal tonnage T_R increases.

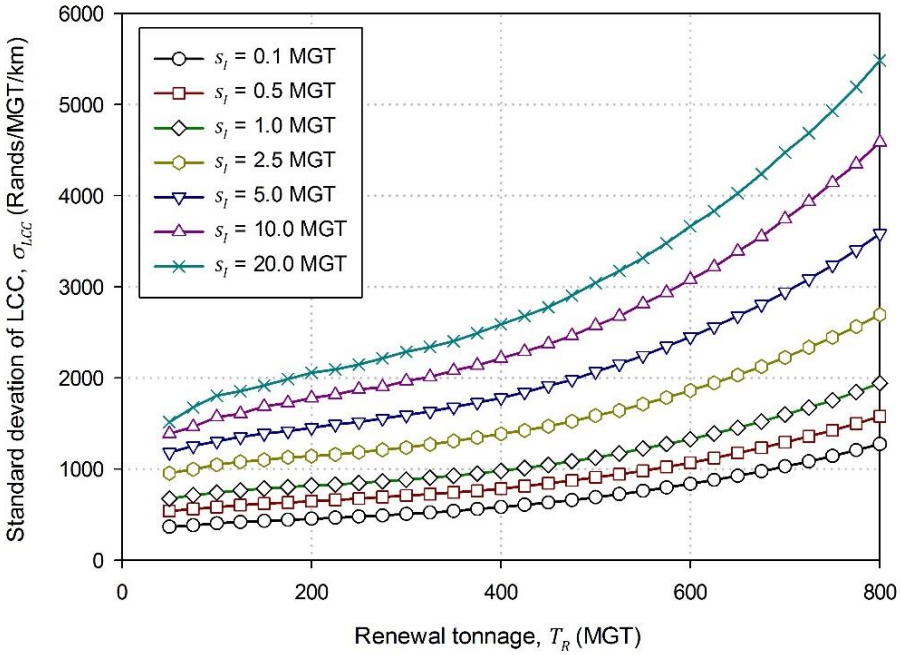

Figure 7. Influence of renewal tonnage T_R on LCC uncertainty σ_{LCC} for varying inspection interval lengths s_I

In Figure 7 the LCC uncertainty at a fixed renewal tonnage appears to be consistently larger for a larger inspection interval length s_I. To illustrate this behaviour, Figure 8 shows plots of LCC uncertainty σ_{LCC} versus inspection interval length s_I for varying renewal tonnages T_R. It is evident that for a fixed renewal tonnage T_R the LCC uncertainty σ_{LCC} increases for an increase in inspection interval length s_I. Furthermore, the behaviour in Figure 8 appears to be asymptotic, approaching a constant level of uncertainty at an infinitely large inspection interval length.

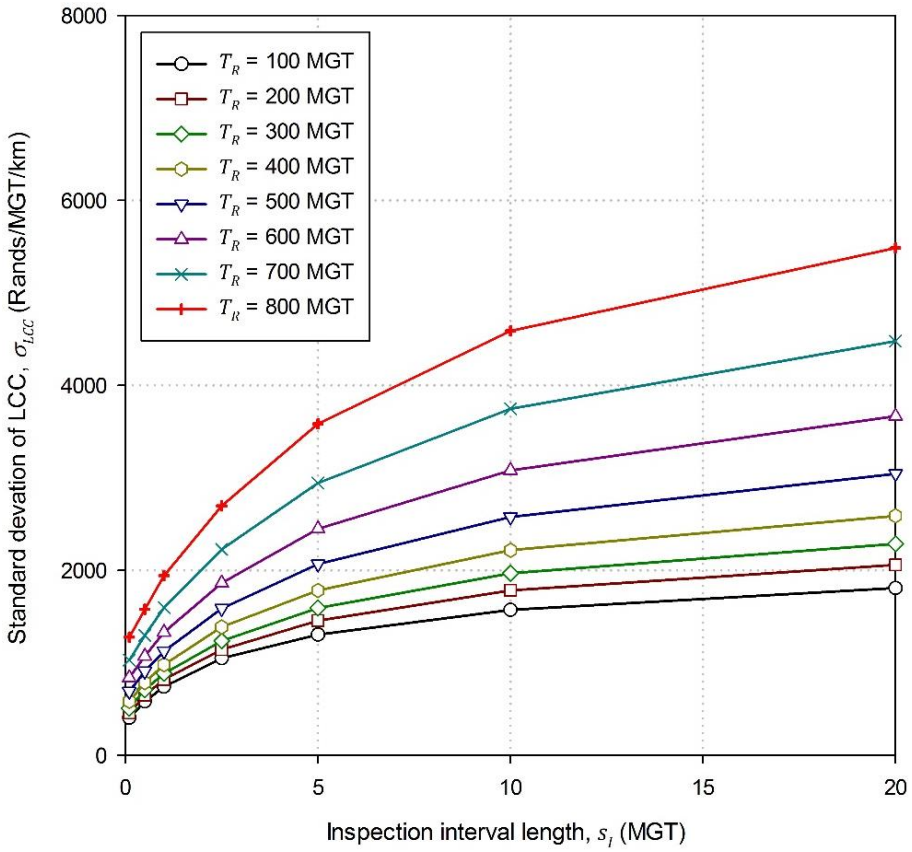

Figure 8. Influence of inspection interval length s_I on LCC uncertainty σ_{LCC} at varying renewal tonnages T_R

The uncertainty in the LCC originates from the uncertainty related to the arrival and detection of defects. Deterministic cost components such as the renewal cost c_R, inspection cost c_I and grinding cost c_g do not contribute to the uncertainty in the LCC. However, the planned and unplanned maintenance costs are affected by the arrival, detection and maintenance of defects and thus are responsible for the uncertainty in the LCC.

The combined maintenance cost $c_{LCC_{combined}}$ is defined as being equal to the planned maintenance cost c_{LCC_p} plus the unplanned maintenance cost c_{LCC_f}.

Figure 9 (a) and (b) shows the planned σ_{LCC_p}, unplanned σ_{LCC_f} and combined $\sigma_{LCC_{combined}}$ maintenance cost uncertainty as a function of renewal tonnage for an inspection interval length s_I = 0.5 and 10.0 MGT respectively. It can be seen that the combined maintenance cost uncertainty $\sigma_{LCC_{combined}}$ is not a simple summation of the two underlying uncertainties. Rather, the combined maintenance cost uncertainty is influenced by the ratio of planned to unplanned maintenance activities as well as the relative cost thereof. It is evident from Figure 9 that the behaviour of the combined maintenance cost uncertainty $\sigma_{LCC_{combined}}$ tends more towards the behaviour of the planned maintenance cost uncertainty σ_{LCC_p} for an inspection interval length of s_I = 0.5 MGT and more towards the unplanned maintenance cost uncertainty σ_{LCC_f} for the larger inspection interval length s_I = 10.0 MGT.

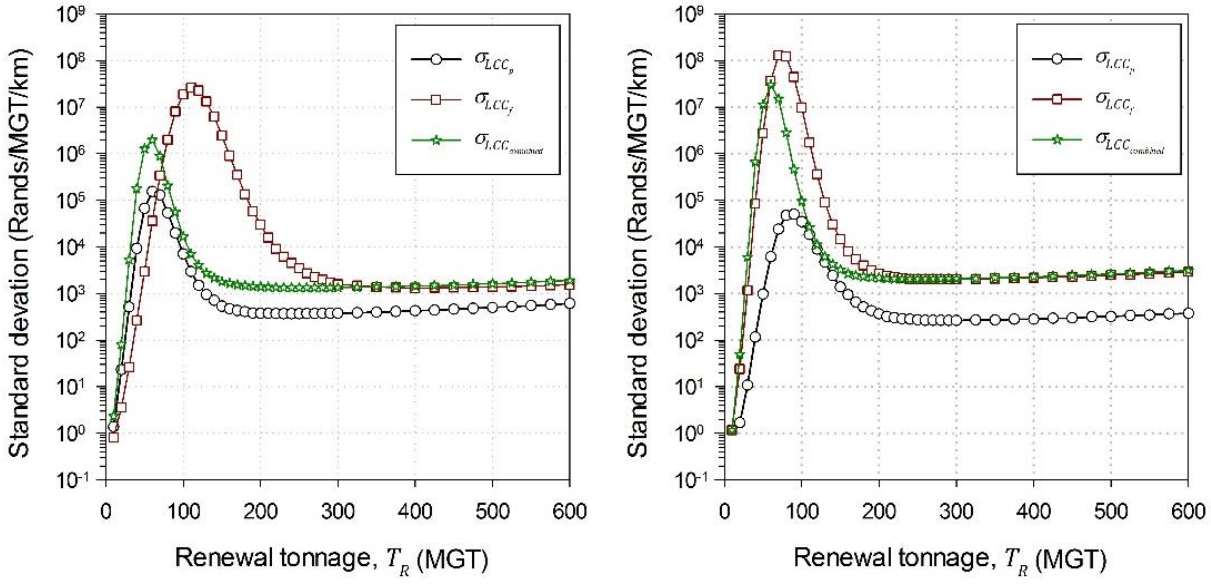

Figure 9. Planned σ_{LCC_p}, unplanned σ_{LCC_f} and combined $\sigma_{LCC_{combined}}$ maintenance cost uncertainty for (a) s_I = 0.5 MGT and (b) s_I = 10.0 MGT

CONCLUSIONS

The objective of the study was to identify trends and quantify the uncertainty in the LCC associated with the maintenance and renewal of the rail of a railway track. A numerical model was developed using MATLAB and incorporating Monte Carlo simulation to adequately reflect the influence of the variability in reliability and maintainability parameters on the uncertainty of the final estimated LCC.

It was found that Monte Carlo simulation can adequately estimate the uncertainty in the LCC for a given renewal tonnage and set of input conditions. With proper quantification of the uncertainty in the LCC, infrastructure managers can make informed decisions with regard to the maintenance and renewal of the rail in relation to the level of risk which they may find acceptable. Furthermore, Monte Carlo simulation relaxes the assumptions otherwise required to attain a closed-form solution. Therefore, the assumption of minimal maintenance was no longer required and new welds could be modelled using perfect maintenance. Also, the hazard rate of FBWs in the system did not have to remain unaffected by maintenance activities as was the case in previous maintenance models.

The mean or expected LCC curve provides useful insights into the influence of maintenance decisions. However, the mean LCC reveals nothing regarding the underlying uncertainty in the LCC and thus does not provide insights into the risks present. The standard deviation of the LCC at a given renewal tonnage was used as a metric to represent uncertainty. It was found that the uncertainty in the LCC increased with an increase in inspection interval length as well as an increase in

renewal tonnage. Furthermore, the proportional contribution of unplanned maintenance cost uncertainty towards the combined maintenance cost uncertainty increased with an increase in inspection interval length. The opposite was found to be true with regard to the contribution of planned maintenance cost uncertainty towards the combined maintenance cost uncertainty.

ACKNOWLEDGEMENTS

Transnet Freight Rail and the Railway Safety Regulator are acknowledged for supporting the research carried out by the Chairs in Railway Engineering and Railway Safety respectively.

FUNDING

This research received no specific grant from any funding agency in the public, commercial, or not-for-profit sectors.

DECLARATION OF CONFLICTING INTERESTS

The authors declare that there is no conflict of interest.

REFERENCES

1. Esveld C. Modern Railway Track. 2nd ed. Zwarthoed-van Nieuwenhuizen D, editor.: Delft University of Technology; 2001.

2. Zoeteman A. Life cycle cost analysis for managing rail infrastructure: concept of a decision support system for railway design and maintenance. European Journal of Transport & Infrastructure Research. 2001; 1(4): p. 391-413.

3. Schlake BW, Barkan CPL, Edwards JR. Train Delay and Economic Impact of In-Service Failures of Railroad Rolling Stock. Transportation Research Record: Journal of the Transportation Research Board. 2011; 2261: p. 124-133.

4. Kumar S, Espling U, Kumar U. Holistic procedure for rail maintenance in Sweden. Proceedings of the Institution of Mechanical Engineers, Part F: Journal of Rail and Rapid Transit. 2008; 222(4): p. 331-344.

5. Reinschmidt A. Wheel and Rail Damage Mechanisms. In Leeper J, Allen R, editors. Guidelines to Best Practices for Heavy Haul Railway Operations. Virginia: Simmons-Boardman Books, Inc.; 2015.

6. Fröhling RD. Wheel/rail interface management in heavy haul railway operations - applying science and technology. Vehicle System Dynamics. 2007; 45(7-8): p. 649-677.

7. Marais JJ, Mistry KC. Rail integrity management by means of ultrasonic testing. Fatigue & Fracture of Engineering Materials & Structures. 2003; 26(10): p. 931-938.

8. Kumar S. A Study of the Rail Degradation Process to Predict Rail Breaks. Licentiate Thesis. Luleå: Luleå University of Technology; 2006.

9. Cannon DF, Edel KO, Grassie SL, Sawley K. Rail defects: an overview. Fatigue & Fracture of Engineering Materials & Structures. 2003; 26(10): p. 865-886.

10. Zhao J, Chan AHC, Roberts C, Stirling AB. Assessing the economic life of rail using a stochastic analysis of failures. Proceedings of the Institution of Mechanical Engineers, Part F: Journal of Rail and Rapid Transit. 2006; 220(2): p. 103-111.

11. Moubray J. Reliability-centered Maintenance. 2nd ed. New York: Industrial Press Inc.; 1997.

12. Jeong DY, Tang YH, Orringer O. Damage tolerance analysis of detail fractures in rail. Theoretical and Applied Fracture Mechanics. 1997; 28: p. 109-115.

13. Jablonski D, Tang YH, Pelloux RM. Simulation of railroad crack growth life using laboratory specimens. Theoretical and Applied Fracture Mechanics. 1990; 14: p. 27-36.

14. Department of Defense. Definitions of Terms for Reliability and Maintainability (MIL-STD-721C). Military Standard. Washington:; 1981.

15. Kobayashi H, Mark BL, Turin W. Probability, Random Processes, and Statistical Analysis. 1st ed. New York: Cambridge University Press; 2012.

16. Pham H, Wang H. Imperfect maintenance. European Journal of Operational Research. 1996; 94(3): p. 425-438.

17. Patra AP, Söderholm P, Kumar U. Uncertainty estimation in railway track life-cycle cost: a case study from Swedish National Rail Administration. Proceedings of the Institution of Mechanical Engineers, Part F: Journal of Rail and Rapid Transit. 2009; 223(3): p. 285-293.

18. Zarembski AM. Forecasting of track component lives and its use in track maintenance planning. In International Heavy Haul Conference; 1991; Vancouver. p. 61-67.

19. Roth C. Use of the Weibull Distribution to Predict Rail Defect Occurence Rates. In International Federation of Operational Research Societies 18th Triennial Conference; 2008; Sandton, South Africa.

20. Zhao J, Chan AHC, Stirling AB, Madelin KB. Optimizing Policies of Railway Ballast Tamping and Renewal. Transportation Research Record: Journal of the Transportation Research Board. 2006b; 1943: p. 50-56.

21. Shafiee M, Patriksson M, Chukova S. An optimal age-usage maintenance strategy containing a failure penalty for application to railway tracks. Proceedings of the Institution of Mechanical Engineers Part F: Journal of Rail and Rapid Transit. 2016; 230(2): p. 407-417.

22. Robert CP, Casella G. Monte Carlo Statistical Methods. 2nd ed. Casella G, Fienberg S, Olkin I, editors. New York: Springer; 2004.

23. Moore DS. Tests of Chi-Square Type. In D'Agostino RB, Stephens MA, editors. Goodness-of-fit Techniques. 1st ed. New York: Marcel Dekker, Inc.; 1986. p. 63-95.